Published in final edited form as:
Inorg Chem. 2013 December 16; 52(24): 13833–13848. doi:10.1021/ic402236f.

Synthetic Cluster Models of Biological and Heterogeneous Manganese Catalysts for O_2 Evolution

Emily Y. Tsui, **Jacob S. Kanady**, and **Theodor Agapie***
Division of Chemistry and Chemical Engineering, California Institute of Technology, Pasadena, California 91125

Abstract

Artificial photosynthesis has emerged as an important strategy toward clean and renewable fuels. Catalytic oxidation of water to O_2 remains a significant challenge in this context. Mechanistic understanding of currently known heterogeneous and biological catalysts at a molecular level is highly desirable for fundamental reasons as well as for the rational design of practical catalysts. This article discusses recent efforts in synthesizing structural models of the oxygen-evolving complex (OEC) of photosystem II (PSII). These structural motifs are also related to heterogeneous mixed metal oxide catalysts. A stepwise synthetic methodology was developed toward achieving the structural complexity of the targeted active sites. A geometrically restricted multinucleating ligand, but with labile coordination modes, was employed for the synthesis of low oxidation state trimetallic species. These precursors were elaborated to site-differentiated tetrametallic complexes in high oxidation states. This methodology has allowed for structure-reactivity studies that have offered insight into the effects of different components of the clusters. Mechanistic aspects of oxygen-atom transfer and incorporation from water have been interrogated. Significantly, a large and systematic effect of redox-inactive metals on the redox properties of these clusters was discovered. With the pK_a of the redox-inactive metal-aqua complex as a measure of Lewis acidity, structurally analogous clusters display a linear dependence between reduction potential and acidity; each pK_a unit shifts the potential by ca. 90 mV. Implications for the function of the biological and heterogeneous catalysts are discussed.

1. Introduction

Photosynthesis, the sunlight-powered process by which plants, algae, and cyanobacteria convert carbon dioxide and water into carbohydrates and O_2, is responsible for the dioxygen in Earth's atmosphere.[1-3] Light-driven water oxidation occurs at photosystem II (PSII), a membrane protein assembly that absorbs four photons to sequentially oxidize a $CaMn_4O_5$ cluster, known as the water oxidizing complex (WOC) or the oxygen-evolving complex (OEC), through a sequence of S_n states called the Kok cycle.[4-5] At the most oxidized state, S_4, dioxygen is released. Water acts as the source of the electrons that are transferred through a series of cofactors and stored as NADPH.[1-3] The reducing equivalents and proton gradient generated by photochemical water oxidation power carbon dioxide fixation and other processes of life. Overall, solar energy is converted and stored as chemical bonds. Many efforts have been devoted to structural, spectroscopic, and biochemical studies of the OEC because understanding how plants form oxygen from water will have implications for designing artificial catalysts for solar fuels. Heterogeneous metal oxide water oxidation catalysts have been proposed to perform their function at discrete multimetallic sites reminiscent of the OEC.[6-10] Artificial water oxidation catalysts have been prepared from

*Corresponding Author agapie@caltech.edu.

Ca-doped manganese oxide materials to mimic the composition of the OEC, despite the limited structural understanding.[8,11-14] Other mixed metal oxides have intriguing catalytic properties, both for water oxidation and oxygen reduction.[15-19] Metal oxides are also important as battery materials.[20-23] Access to and study of well-defined metal oxide clusters structurally analogous to the active sites of these catalysts are expected to provide insight into the interactions between different types of metals and their effect on the properties of the cluster and the catalytic material.

1.1 Structural and mechanistic studies of the OEC

X-ray absorption spectroscopy (XAS)[24-28] and electron paramagnetic resonance (EPR)[29-34] methods have been employed to identify oxidation state, electronic structure, and coordination environment changes during the S-state progression. Recent single crystal X-ray diffraction (XRD) studies have shown that the OEC consists of a $CaMn_3O_4$ cubane cluster with the fourth "dangler manganese" center bridged via oxide moieties (Figure 1).[35-36] Subsequent computational studies, however, have suggested that this structure corresponds to a more reduced manganese cluster due to X-ray damage,[37-38] consistent with previous studies on X-ray-induced reduction,[39] or to an equilibrium of multiple structural forms at similar energies.[40-41] More open cubane structures of the S_2 state have been proposed by calculations that are consistent with OEC geometries advanced from EPR and XAS studies (Figure 2).[28,31,41-43]

Due to these uncertainties in the structural details of the S states of the OEC, the mechanism of O–O bond formation during water oxidation remains controversial. Isotopic labeling studies using mass spectrometry and magnetic resonance techniques have been used to analyze substrate water exchange rates with bulk water within the OEC.[44-46] Based on these studies and spectroscopic data, several mechanisms for O–O bond formation have been proposed. These proposals differ in the nature and location of the substrate oxo moieties that undergo O–O bond formation to generate O_2. Early proposals, such as the manganese-only adamantane and the double-pivot mechanisms, proved incorrect based on structural grounds.[47-49] Heterolytic pathways involve a water or hydroxide ligand bound to Ca^{2+} attacking a Mn(V) oxo or Mn(IV) oxyl.[50-52] Other mechanisms have suggested that a terminal oxyl reacts with a bridging oxido moiety via a radical mechanism (Figure 3).[42,53-54] Distinguishing the different mechanisms through computational and experimental studies remains a challenge.

The role of calcium, which is known to be necessary for activity, is an unclear aspect of water oxidation at the OEC.[57-60] In particular, the association of Ca^{2+}, a redox-inactive metal, with an active site that performs a multielectron redox transformation is puzzling and departs from other roles of Ca^{2+} in biological systems. XAS and XRD studies have revealed that Ca^{2+} is bridged by oxido moieties to the manganese centers in the OEC, but does not function solely as a structural component. Substitution of other metal ions for Ca^{2+} leads to inhibition of catalysis, except for Sr^{2+}, which recovers activity, albeit to a lower extent (ca. 40%).[3,57,61] The Sr^{2+}-substituted OEC shows subtle changes in geometry (XAS)[62] and electronic structure (EPR)[63] compared to the native $CaMn_4O_x$ cluster. The ability of Sr^{2+} and Ca^{2+} to maintain catalysis has been explained in terms of their similar Lewis acidities in the context of binding and activating a water substrate.[50,52,64-65] Size or charge effects were deemed secondary, as Cd^{2+}, an ion with the same ionic radius as Ca^{2+}, does not support water oxidation.[3,64] Others have proposed that Ca^{2+} affects proton coupled electron transfer and the redox properties of the cluster, possibly via interactions through a H-bond network with the neighboring tyrosine residue or by affecting the protonation state of a coordinated water molecule.[26,66-67] Despite detailed biochemical and spectroscopic studies, the role of calcium in the OEC remains under debate. Synthetic models to complement these investigations were extremely scarce and not structurally accurate, until recently.

1.2 Heterogeneous metal oxides as water oxidation catalysts

Heterogeneous manganese-containing materials have been studied for their water oxidation activities, and parallels have been drawn to the biological system. Although undoped manganese oxides have been demonstrated to catalyze water oxidation at low efficiencies, addition of calcium greatly increases the reaction efficiency, raising the possibility that the mechanism of dioxygen formation is related to that of the biological OEC.[11,14] XAS studies of these materials determined that the Mn centers are of the +3 and +4 oxidation state, and that the redox-inactive ions may be bridged to the Mn centers by oxido moieties in similar MMn_3O_4 cuboidal subsites as in the OEC.[8-9] These results suggest that further understanding of PSII may allow for the rational design of more efficient heterogeneous water oxidation catalysts. Beyond manganese water oxidation catalysts, the proposed catalytic site of cobalt oxide has been illustrated with redox-inactive cations at positions reminiscent of the Ca^{2+} position in the OEC (Figure 2),[6-7] (although alkaline metals were not detected by EXAFS).[68]

1.3 Synthetic manganese clusters

Synthetic biomimetic complexes have been targeted to supplement the structural, spectroscopic, and mechanistic studies of biological systems while at the same time exploring the possibilities of catalysis. Structural and functional modeling of the OEC has been challenging, in particular due to the propensity of the oxido moieties to bridge and generate oligomeric structures in uncontrolled fashion. Many mononuclear, dinuclear, trinuclear, and tetranuclear manganese complexes have been prepared as models and have been extensively reviewed in the literature.[2,69-78] These high oxidation state manganese oxido complexes are often synthesized by spontaneous self-assembly by oxidation of manganese(II) salts; for these compounds, the choice of oxidant is crucial. Bridging oxides are known to stabilize higher oxidation state Mn centers, but also to significantly affect the geometry, Mn–Mn distance, and magnetic exchange of these compounds.[69] A second important aspect is the choice of ancillary ligands. These ligands, often polydentate O- or N-donors, are chosen to limit aggregation and to stabilize certain oxidation states. Manganese carboxylate chemistry especially has been heavily studied, due to the carboxylate-containing residues in the OEC binding site.[72] In the following section, selected examples of manganese oxide clusters will be discussed, with emphasis on tetramanganese complexes and heterometallic complexes as they are particularly relevant to the composition of the OEC.

Mixed-valent $Mn^{III,IV}_2$ bis(μ-oxo) dimers stabilized by polydentate N-donor ligands have been of particular interest in OEC biomimetic chemistry since they were first prepared and studied for their magnetic exchange coupling properties (Fig. 4, **A**).[79-81] Although these lower nuclearity complexes were clearly not structural mimics of the tetramanganese OEC cluster, they were heavily studied because of the Mn–Mn distance of 2.7 Å, which is similar to distances in the OEC measured by XAS studies,[82] as well as a multiline EPR signal that is similar to the multiline signal observed for the S_2 state of the OEC.[81,83] From a structural perspective, a dimer-of-dimers model was proposed for the S_2 state OEC based on these observations,[26,84] and synthetic models were prepared (Fig. 4, **B**).[85-87] The dimer-of-dimers model was later shown to be inconsistent with EPR spectroscopic measurements that support a 3+1 arrangement of the manganese centers.[31] From a functional aspect, Brudvig and co-workers have used a terpyridine-supported $Mn^{III,IV}_2$ bis(μ-oxo) complex for water oxidation using oxone or hypochlorite as the oxidant.[88-89] Based on kinetic and isotope-labeling studies, a terminal $Mn^{V}O$ moiety was proposed as an intermediate for dioxygen formation.[90]

One of the earliest high oxidation state tetramanganese oxido clusters, prepared by Christou and co-workers, was a [Mn_4O_2] complex in which the Mn centers are in a "butterfly" arrangement (Fig. 4, **C**).[91-92] This structure was proposed to participate in the Kok cycle through a "double-pivot" mechanism to rearrange to more cubane-like structures.[48] Tetramanganese cubane structures had previously been proposed as intermediates in the water oxidation pathway of the OEC,[48-49] but were not synthetically accessed until Christou and coworkers isolated an acetate-bridged tetramanganese trioxido chloride cubane complex (Fig. 4, **D**).[93] A diarylphosphinate-supported tetraoxido $[Mn_4O_4]^{n+}$ cubane variant was later isolated by Dismukes and coworkers via the spontaneous assembly of mononuclear or dinuclear manganese precursors (Fig. 4, **E**).[94-95] These clusters are proposed to be stabilized by π-interactions between the aryl groups of the phosphinate ligands.[95] The diarylphosphinate stabilized system was also proposed to photoelectrochemically oxidize water to dioxygen when embedded in a Nafion film;[96] however, an amorphous manganese oxide material was later found to be the active catalyst.[97] Adamantane-type tetramanganese clusters have also been described (Fig. 4, **F**).[98-99]

One of the most important, but least explored, problems in preparing accurate structural models of the OEC has been the incorporation of calcium in the clusters. Heterometallic manganese clusters are relatively rare, and have been isolated as molecular species only in recent years.[100-106] The first high oxidation state manganese cluster with incorporated calcium, $[Mn_{13}Ca_2O_{10}(OH)_2(OMe)_2(O_2CPh)_{18}(H_2O)_4]\cdot 10MeCN$ (Fig. 5, **G**) was prepared by Christou and coworkers from calcium salts such as $Ca(NO_3)_2\cdot 4H_2O$, $Ca(ClO_4)_2$, or $Ca(O_2CPh)_2$ and $(NBu_4)[Mn_4O_2(O_2CPh)_9(H_2O)]$.[100] Although this is a high nuclearity [$Mn_{13}Ca_2$] cluster much larger than the [Mn_4Ca] motif found in PSII, one portion resembled the OEC in that it had a $CaMn_3O_4$ cubane subunit with a fourth manganese center bridged to the cluster via an oxide moiety. A similar compound with Sr^{2+} rather than Ca^{2+} was also later isolated and studied.[101,107] Powell and coworkers used a chelating Schiff base ligand to generate $CaMn_4$ clusters, though with only one incorporated oxide moiety (Fig. 5, **H**).[102-103] A heterometallic polymeric material with a Mn_3O unit in proximity to a Ca^{2+} center was isolated (Fig. 5, **I**).[108] To the authors' knowledge, only three other Mn/Ca clusters had been reported and characterized by crystallography prior to 2011, all with no bridging oxido ligands: a Mn_4 metallacrown moiety with a Ca^{2+} center coordinated to one side of the crown and chelated by carboxylates;[109] a $Mn^{II}{}_4Ca_2$ cluster with bridging alkoxides;[110] and a Mn_3NaCa coordination polymer.[111] The oxidation state of Mn in these compounds varies from mixed-valent $Mn^{II}/Mn^{III}/Mn^{IV}$ or Mn^{II}/Mn^{III} to all-Mn^{II} or all-Mn^{III}. These synthetically novel heterometallic compounds demonstrate that although the self-assembly strategy is structurally very versatile, control of oxidation state, oxide incorporation, and level of aggregation to form the desired molecular model clusters remains challenging.

A complementary approach reported concurrently with our work on clusters investigated the effects of Ca^{2+} and other redox-inactive metals in heterometallic binuclear complexes. Borovik and co-workers exploited a tripodal tris(sulfonamide) ligand framework to access complexes of transition metals such as Mn, Fe, and Co associated via a bridging hydroxide with Ca^{2+}, Sr^{2+}, and Ba^{2+} centers that are also coordinated by two sulfonamide oxygen donors (Fig. 5, **J**).[104,106,112] The redox-inactive metal was reported to affect the reduction potentials of the complexes as well as the rate of reaction with O_2. Although not structurally characterized, Sc^{3+} association to $Mn^{I\text{-}V}O$ moieties have been reported by Fukuzumi, Nam et al. to affect the reduction potential as well as reactivity, including the rates of electron transfer, O-atom transfer, and H-atom abstraction.[113-114] Related effects have been observed for $Fe^{IV}O$ moieties coordinated with redox-inactive metals, the Sc^{3+} version being structurally characterized.[115-116] Valence tautomerism was reported by Goldberg, de Visser, et al. for $Mn^{V}O$-porphyrinoid complexes upon addition of Zn^{2+}, which affected redox and H-atom transfer chemistry.[117] These elegant studies show clearly that redox-inactive metals

significantly affect the chemistry of transition metal-oxo species. Implications to the chemistry of the OEC have been proposed; however, more structurally accurate cluster models of the OEC remain very desirable to interrogate the effects on the physical properties and chemical reactivity of the complexes by changing various aspects such as structure, oxidation state, nature of redox-inactive metal, and number of oxido moieties.

2. Synthesis of Site-Differentiated Multinuclear Manganese Complexes

Access to models of the active sites in biological and heterogeneous catalysts for water oxidation represents a significant synthetic challenge for several reasons, including the relatively large number of atoms, the presence of two types of metals, metal lability, and cluster asymmetry. In one possible strategy for modeling the OEC, outlined in a retrosynthetic fashion (Scheme 1), the “dangler” is attached late in the synthesis to a $CaMn_3O_4$ cubane structure. Accessing the simpler and higher-symmetry $CaMn_3O_4$ cubane presents the challenge (vide supra) of incorporating two types of metals bridged by oxides in the same cluster in a 3:1 ratio. A precursor to such species was envisioned in a trimetallic manganese complex.

This synthetic approach is reminiscent of Holm’s methodology for the preparation of site-differentiated cuboidal iron-sulfur clusters.[118-122] Site-differentiated Fe_4S_4 cubanes are found in several metalloenzymes, with one of the supporting cysteinyls bridged to another metal fragment. In order to model such moieties, a semirigid tris-thiolate ligand was employed to support three of the four metals of the cubane moiety. Incomplete iron sulfur clusters, Fe_3S_4, supported by this trinucleating ligand could be isolated and utilized as precursors to homo- and hetero-metallic Fe_3MS_4 moieties (Scheme 2).

Toward heterometallic manganese oxido complexes, preformed trimanganese clusters were targeted that could be oxidized with concomitant addition of a fourth metal center. A multinucleating ligand based upon a semi-rigid 1,3,5-triarylbenzene framework was synthesized, with the three peripheral aryl groups functionalized by a dipyridylmethanol moiety (Scheme 3). The lability of the dipyridylalkoxymethyl moiety is well documented in the coordination chemistry of dipyridylketone and the *gem*-diol or hemiacetal form thereof, which chelate and bridge metal ions in a wide variety of binding modes.[123] Such coordinative flexibility was expected to support the formation of different types of clusters on the ligand architecture. Additionally, these donor moieties were expected to support high oxidation state metal centers and be relatively stable to oxidative reaction conditions.

Ligand H_3L (Scheme 3) was prepared on a multigram scale in two synthetic steps from commercially available materials. Lithium-halogen exchange of 1,3,5-tri(2′-bromophenyl)benzene, prepared by cyclization of 2-bromoacetophenone, followed by addition of three equivalents of di(2-pyridyl)ketone affords H_3L in approximately 40% yield over two steps. Compound H_3L was treated with divalent transition metal salts (M^{2+} = Mn^{2+}, Fe^{2+}, Co^{2+}, Ni^{2+}, Cu^{2+}, Zn^{2+}) in the presence of base to form trinuclear complexes. The solid-state structures of these compounds show that the ancillary functionalized triarylbenzene ligand binds the three metal centers in the same fashion, independent of the nature of the metal. The three metals are bridged by μ-alkoxides, and pyridyl groups from each arm of the ligand framework coordinated to adjacent metals (Scheme 3, M = Mn^{2+}, Figure 6).[124-125] Notably, these complexes are stable in the presence of water. Except for the zinc complex, these complexes all have paramagnetically shifted ^1H NMR spectra with diagnostic peaks that allow monitoring of reaction progress and identification of target products. The trinuclear clusters are capped by the counterions from the initial metal salts. The trimanganese(II) tris(acetate) compound, $LMn_3(OAc)_3$ (**1**), was selected as a starting platform for further oxidative functionalization. Compound **1** provides three manganese(II)

centers poised for oxidation and proximally constrained by the ligand framework and bridging alkoxide moieties; furthermore, the acetate ions can serve as ancillary ligands to bridge to additional metal centers.

2.1 Synthesis of Mn_4O_x complexes

Oxidative incorporation of a fourth metal to **1** was studied with various manganese precursors targeting tetramanganese clusters. In this context, permanganate can act as the source of the fourth metal equivalent and oxide moieties, and as the oxidant. Treatment of **1** with two equivalents of $^nBu_4NMnO_4$ leads to the isolation of a tetramanganese tetraoxido cubane cluster, $LMn^{III}_2Mn^{IV}_2O_4(OAc)_3$ (**2**) in 30% isolated yield (Scheme 4; Figure 7).[126] The relatively low yield is likely due to the unbalanced nature of the reaction.

Complex **2** contains a Mn_4O_4 cubane unit, with overall charge and bond lengths consistent with $Mn^{III}_2Mn^{IV}_2$ oxidation state. To accommodate such a drastic change in the cluster structure, the acetates and dipyridyl alkoxide units change binding modes from those observed in **1**. The alkoxides shift from bridging to terminal coordination, three of the pyridyl donors decoordinate and the three acetates form κ^2-bridges across three cubane faces. Complex **2** is *pseudo*-C_3 symmetric. One previous class of Mn_4O_4 cubane complexes with only μ_3-oxido donors has been isolated (**E**), supported by diarylphosphinate bridging ligands.[94] Christou and coworkers have published extensively on $Mn^{III}_3Mn^{IV}O_3X$ cubanes ($X=Cl^-$, I^-, F^-, N_3^-, O_2CR^-, OMe^-, and OH^-).[127-131]

With **1** as precursor, separation of the oxidizing and oxygen equivalents from the metal source was explored, thus expanding the parameter space and providing access to a wider range of tetrametallic complexes. Using potassium superoxide as the oxidant and oxygen source while varying the manganese salt—$Mn(OAc)_2$ *vs.* $Mn(OTf)_2$—and solvent afforded a series of tetramanganese complexes varying in oxido content and oxidation state from μ_4-oxido $Mn^{II}_3Mn^{III}O$ (**3**) $Mn^{II}_2Mn^{III}_2O$ (**4**) complexes, to a dioxido $Mn^{II}_2Mn^{III}_2O_2$ complex (**5**) and partial cubane $Mn^{III}_4O_3$ complex (**6**) (Scheme 4, Figure 7).[132]

In **3** and **4**, the ligand framework coordinates three manganese centers as in **1**, but now a μ_4-oxido and the three acetates bridge the three basal manganese centers to a fourth, five-coordinate manganese center (Figure 7). The tetrahedral μ_4-oxido is a common motif throughout manganese cluster chemistry,[76] and is also a common motif in our work with the L^3–framework. For dioxido complex **5**, a μ_4-oxido bridges the four manganese centers as in **3**. Additionally, a second μ_2-oxido bridges one basal Mn and the apical Mn, forming a $Mn^{III}_2O_2$ diamond core. Complex **5** reacts with dioxygen, formally reducing it by four electrons over days to generate cubane complex **2**, indicating that O_2 reactivity is possible in these systems. For complex **6**, as oxido content increases from two to three, the binding mode of L^{3-} changes to that of **2**, with terminal alkoxides and only three coordinated pyridines. Comparison of the electrochemical properties of **2** and **6** shows one oxidation and one reduction event for each, with differences of less than 150 mV between the two compounds, despite a difference of two units between the metal oxidation states of the two species. This behavior is explained in terms of neutralization of charge buildup on the cluster by incorporation of an O^{2-} donor.[133] This redox leveling of the cluster upon formal water incorporation and deprotonation is relevant to the OEC, as the oxidizing equivalents come at the same potential for all four oxidations during catalysis to generate O_2.

Cationic $Mn^{III}_2Mn^{IV}_2$ cubane complexes such as **7** were prepared by reaction of **2** with one equivalent of trimethylsilyl triflate, followed by addition of neutral Lewis bases. Such lower symmetry species that have one of the Mn_2O_2 faces of the cubane free of anionic ligands, are synthetically important toward accessing clusters with a fifth dangling metal similar to the OEC.

Complexes **2** through **6** span six oxidation states, with two more—Mn^{II}_4 and $Mn^{III}Mn^{IV}_3$—accessible electrochemically. The ability of the present multinucleating ligand architecture to support different binding modes is instrumental for accessing the wide span of metal oxidation states and oxido content. Clusters displaying low oxidation state Mn^{II} centers are coordinated by nine donors from L, binding to twelve coordination sites (counting three μ-alkoxides) while the higher oxidation state species, displaying Mn^{III} and Mn^{IV}, require only six donors (Figure 8). The switch in coordination mode is likely due to the strong Mn-oxido bonds that lead to the displacement of the pyridine and μ-alkoxide donors. The present compounds suggest that donor flexibility is an important factor in the design of ligands for clusters in multielectron chemistry involving transfers of oxygenous moieties. Although the binding mode varies, the ligand set changes little other than the inclusion of oxido ligands, paralleling the photoassembly of the OEC, from four free Mn^{II} ions to the active Mn_4CaO_x cluster.

2.2 Synthesis of $CaMn_3O_x$ complexes

To access heterometallic complexes structurally related to the OEC, Ca/Mn oxido clusters of various oxidation state and oxido content were prepared using a similar approach to that used for homometallic complexes **3**-**6**. The triflate salt was employed as the source of Ca^{2+}, and PhIO or superoxide were used as the sources of oxygen and oxidizing equivalents. Treatment of a THF mixture of **1** and $Ca(OTf)_2$ with PhIO forms the purple compound $[LMn_3O(OAc)_3]_2Ca(OTf)_2$ (**8**), in which each trimanganese moiety has been oxidized to form a $[Mn^{III}_2Mn^{II}O]$ cluster; two $[Mn^{III}_2Mn^{II}(\mu_3\text{-}O)]$ moieties are bridged by acetate ligands to a calcium center that has no interaction with the oxido group (Scheme 5).[126] In the structure of **8**, as in compounds **1**, **3**, **4**, and **5**, the alkoxide moieties of the multinucleating ligand framework bridge the Mn centers in the basal trimanganese core, and all pyridyl donors are coordinated. Isolation of **8** demonstrated the viability of our strategy of oxidative functionalization of **1** with non-manganese metal sources. More oxidized complexes, relevant to the oxidation states proposed for the S states formed during the Kok cycle, were targeted.

Treatment of **8** with one equivalent of $Ca(OTf)_2$ and two of PhIO in 1,2-dimethoxyethane (DME) forms the dioxido complex $[LCaMn^{III}_2Mn^{IV}O_2(OAc)_2(DME)(OTf)][OTf]_2$ (Scheme 5, [**9**-Ca(DME)(OTf)][OTf]$_2$).[134] Compound [**9**-Ca(DME)(OTf)][OTf]$_2$ can also be prepared directly from **1** by treatment with $Ca(OTf)_2$ (1.5 equiv) in DME with PhIO (2 equiv). In [**9**-Ca(DME)(OTf)][OTf]$_2$, the Ca^{2+} center is bridged to the more oxidized $[Mn^{IV}Mn^{III}_2]$ unit via two acetate ligands as well as bridging μ_2- and μ_4-oxido moieties (Figure 9 left). The Ca^{2+} center is further coordinated by a DME ligand and a κ_1-trifluoromethanesulfonate anion, with two triflate anions remaining outer sphere. The DME and triflate ligands on Ca^{2+} can be substituted with other donors. For example, upon exposure to water, the tris(aqua) variant $[\mathbf{9}\text{-}Ca(OH_2)_3]^{3+}$ was isolated and structurally characterized (Figure 9 right). Compound [**9**-Ca(DME)(OTf)][OTf]$_2$ reacts with decamethylferrocene ($FeCp^*_2$) to generate the isostructural one-electron reduced Mn^{III}_3 compound [**10**-Ca(DME)(OTf)][OTf]. The coordination environments of complexes $[\mathbf{10}\text{-}Ca(DME)(OTf)]^+$ (Mn^{III}_3) and $[\mathbf{9}\text{-}Ca(DME)(OTf)]^{2+}$ ($Mn^{III}_2Mn^{IV}$) are identical, with only slight changes in the bonds lengths due to the changes in the oxidation state at manganese. Treatment of [**10**-Ca(DME)(OTf)][OTf] with AgOTf regenerates [**9**-Ca(DME)(OTf)][OTf]$_2$. Compounds **9** and **10** are structurally related to the tetramanganese dioxido complex **5**, but with more oxidized manganese centers.

To form a more oxidized $CaMn_3$ cluster in analogy to the formation of the all-manganese clusters **2** or **7**, a mixture of **1** and $Ca(OTf)_2$ was treated with excess KO_2 in THF to afford a tetraoxido cubane compound $LCaMn^{IV}_3O_4(OAc)_3(THF)$ (**11**-Ca). Compound **11**-Ca can

also be isolated by the oxidation of [**9**-Ca(DME)(OTf)]$^{2+}$ with sodium peroxide or the oxidation of **8** with potassium superoxide, indicating that these partially oxidized species could be intermediates on the path to generating the cubane from low oxidation state precursors, as in biological photoactivation. The structure of **11**-Ca is closely related to that of **2**, with four μ_3-oxido moieties bridging the four metals, though **11**-Ca is more oxidized than **2** and contains three Mn^{IV} centers. As with **2**, the coordination mode of the alkoxide donors in L has shifted from bridging to terminal, and each manganese center is coordinated by a single pyridyl donor and κ_2-bridging acetate groups (Figure 10a). The Ca^{2+} center is 7-coordinate with a THF molecule in the apical position. Compound **11**-Ca represents the first accurate model of the cubane subsite of the OEC; this discrete cluster shows that rational synthetic methodologies can be developed toward accessing models of one of the most complex inorganic active sites known in biology. Comparison of the structure of **11**-Ca to EXAFS and XRD studies of the OEC core (Figure 10b) shows that the Mn-Mn and Mn-Ca distances are similar; the Mn-Mn distances in **11**-Ca are about 2.8 Å, longer than the 2.7 Å vectors observed by EXAFS,[28] but similar to the 2.8 and 2.9 Å Mn-Mn distances observed in the recent XRD structure.[36] The Ca-Mn distances in **11**-Ca are slightly shorter (3.23 Å) than the 3.3–3.5 Å distances calculated by EXAFS studies, likely due to the higher oxidation state and number of bridging acetate ligands in **11**-Ca.[28] The structure of **11**-Ca is also very similar to a related pivalate-supported [$Ca_2Mn_3O_4$] cluster recently reported by Christou and co-workers containing a similar [$CaMn^{IV}{}_3O_4$] subsite (Figure 10c).[105] In that example, the Ca-Mn distances are slightly longer (3.4 Å), with shorter Mn-Mn distances (2.73, 2.76, and 2.86 Å). The authors suggest that the asymmetry of the [$Ca_2Mn_3O_4$] cluster distorts the structure, making it more analogous to the structure of the OEC. Finally, $CaMn_3O_4$ cubane subsites have been proposed in heterogeneous systems based on XAS studies (Figure 10d).[9] In these systems, EXAFS data revealed average Mn-Mn distances of ca. 2.88 Å, again similar to the values observed for model compound **11**-Ca. On-going spectroscopic studies of **11-Ca** and related species are expected to provide insight relative to the properties of the OEC. Both synthetic systems displaying the $CaMn^{IV}{}_3O_4$ moiety show ferromagnetic coupling.[105,135]

2.3 Synthesis of heterometallic Mn_3MO_x complexes

The rational, step-wise synthesis used in the present series of Ca/Mn mixed metal oxido complexes allows for controlled, targeted changes to their structure and metal content. Given the outstanding questions regarding the role of Ca^{2+} in the OEC, synthetic targets that interrogate the effect of changing the nature of the redox-inactive metal in heterometallic clusters are of interest. Such clusters were targeted for both MMn_3O_2 and MMn_3O_4 motifs.

Under similar conditions as for the synthesis of [**9**-Ca(DME)(OTf)]$^{2+}$, Na^+-, Sr^{2+}-, and Y^{3+}-substituted dioxido clusters with the same [MMn_3O_2] core can be formed by replacing $Ca(OTf)_2$ with the corresponding metal triflate precursor (Scheme 6).[134] Although the Sr^{2+}-substituted compound [$LSrMn^{III}{}_2Mn^{IV}O_2(OAc)_2(DME)(OTf)]^{2+}$ ([**9**-Sr(DME)(OTf)]$^{2+}$) is analogous to the Ca^{2+} compound, the Y^{3+}-substituted dioxido complex was isolated in the more reduced $Mn^{III}{}_3$ state as [$LYMn^{III}{}_3O_2(OAc)_2(DME)(OTF)]^{2+}$ ([**10**-Y(DME)(OTf)]$^{2+}$), and the Na^+-substituted complex was isolated as a dimer with sodium centers bridged through acetate oxygens rather than coordinated by DME or triflate anions, [$LNaMn^{III}{}_2Mn^{IV}O_2(OAc)_2]_2{}^{4+}$ ([**9**-Na]$_2{}^{4+}$). Analogously to the synthesis of the reduced complex [**10**-Ca(DME)(OTf)]$^+$, the reduced Sr^{2+}-substituted complex [$LSrMn_3O_2(OAc)_2(DME)(OTf)]^+$ ([**10**-Sr(DME)(OTf)]$^+$) was prepared by addition of one equivalent of $FeCp^*_2$ to [**9**-Sr(DME)(OTf)]$^{2+}$. In a complementary synthetic route, treatment of [**9**-Ca(DME)(OTf)]$^{2+}$ with $Zn(OTf)_2$ leads to the Zn-capped dioxido cluster [$LZnMn_3O_2(OAc)_2(CH_3CN)$][OTf] ([**9**-Zn($CH_3CN$)]$^{3+}$) via transmetallation. These

complexes were all characterized by single crystal X-ray diffraction studies, and all maintain a similar [MMn_3O_2] core structure with the same ligand L binding mode.

We also targeted a similar series of heterometallic tetraoxido clusters structurally related to the cubane subsite of the OEC.[136] The Sr-substituted complex LSrM-n$^{IV}_3O_4(OAc)_3$(DMF) (**11**-Sr) was prepared from **1**, $Sr(OTf)_2$, and KO_2 analogously to the synthesis of **11**-Ca (Scheme 7). Related complexes with other metals were not successfully isolated using this method, but transmetallation of **11**-Ca was found to be facile. As such, the corresponding [$MMn^{IV}_3O_4$] complexes were prepared by treatment of **11**-Ca with the metal triflate salt in DMF (Scheme 7, M = Zn^{2+}, Y^{3+}, Sc^{3+}). The Y^{3+}- and Sc^{3+}-substituted complexes are cationic due to the additional positive charge of the redox-inactive metal. The one-electron reduced compound LScMn^{III}Mn$^{IV}_2O_4(OAc)_3$(DMF) (**12**-Sc) was isolated by reduction of [**11**-Sc][OTf] with one equivalent of $FeCp^*_2$. Although the cubane structure is retained, the structural parameters show axial distortion diagnostic of Mn^{III} due to population of a σ-antibonding orbital. All cubane complexes were characterized by XRD studies; they maintain the [MMn_3O_4] cubane geometry of **11**-Ca.

Overall the presented synthetic methodologies are very versatile. They have provided access to a variety of site-differentiated homo- and heterometallic tetranuclear clusters. With these series of compounds in hand, a variety of studies were performed to interrogate the properties of these clusters related to the OEC and proposed active sites of heterogeneous water oxidation catalysts.

3. Insights from studies of manganese clusters

3.1 Mechanism of oxidative water incorporation

Assembly of the OEC from reduced precursors requires oxidative water incorporation to generate the high-oxidation state mixed metal-oxide cluster. Additionally, for each catalytic turnover of the water oxidation reaction the substrate has to be coordinated to the cluster and deprotonated (Figure 3). Site-differentiated clusters provide a convenient platform for studying the mechanism of oxidative water incorporation and oxygen atom transfer.

During the formation of the OEC, called photoactivation,[137] water is deprotonated and incorporated into the manganese cluster at bridging oxido positions. Some proposals for the mechanism of the catalytic water oxidation cycle also suggest oxidative incorporation of substrate water into bridging positions.[56,138] Substrate water exchange studies on the OEC revealed fast (≥ 120 s^{-1} in S_2) and slow (2 s^{-1} in S_2) exchanging substrate waters.[139] These rates are faster than those observed in model systems containing μ_2- and μ_3-oxidos in dinuclear and tetranuclear manganese complexes.[140-142] Some use this distinction to argue that the substrate waters are terminally bound to manganese or calcium throughout the Kok cycle.[55,143] Others have argued that substrate water is indeed incorporated into a μ-oxido position, but is in equilibrium between two sites in the S_1 and S_2 states (Scheme 8, top), thus affording this migrating oxido with a faster exchange rate than those observed in model complexes.[40-41,144]

We studied water exchange and incorporation in homo- and heterometallic cubanes **2**, **11**-Ca, and [**11**-Sc]$^+$. Consistent with literature water exchange studies,[140-142] no exchange of $H_2{}^{18}O$ was observed over hours for these μ_3-oxide ligands.[135] To develop the mechanistic tools for studying the migration of oxide moieties within model clusters, we explored the possibility of interconversion between partial $Mn^{III}_4O_3$ cubane, **6**, and $Mn^{III}_2Mn^{IV}_2O_4$ cubane, **2**. Since **2** and **6** differ by only an oxygen atom, we tested whether these could be interconverted by oxygen-atom acceptors (phosphines, thioethers), oxygen-atom donors (amine oxides, iodosobenzene), and oxidative water incorporation. Treatment of **2** with

PMe_3 quantitatively afforded **6** (Scheme 8). The same reaction using PEt_3 is much slower, suggesting that sterics play an important role. For the reverse reaction, treatment of **6** with PhIO afforded **2**. The heterometallic cubanes **11**-Ca and [**11**-Sc]$^+$ are stable to PMe_3, and no O-atom transfer was observed by NMR spectroscopy. Since [**11**-Sc]$^+$ is more oxidizing than **2** and **11**-Ca, though for an one-electron transfer process (vide infra), the difference in reactivity is consistent with kinetic rather than thermodynamic control for the oxygen-atom transfer reaction. When ligand exchange experiments with d_3-acetate were performed with **2**, **11**-Ca, and [**11**-Sc]$^+$, the acetates scrambled much faster with **2** (statistical mixture in ca. 1 minute) than **11**-Ca and [**11**-Sc]$^+$ (statistical mixture in ca. 1 hour). This difference in rate is not surprising given the presence of Mn^{III} centers in **2** that are labile due to the population of a σ-antibonding orbital, while the heterometallic clusters **11**-Ca and [**11**-Sc]$^+$ have only Mn^{IV} centers.

The reactivity of these cubanes was studied by quantum mechanics. As expected, PMe_3 attack at the bottom position was prohibitively high in energy due to steric interactions with ligand L. For **2**, a transition state was calculated where one acetate decoordinated from a bottom manganese to allow room for the PMe_3 to approach a μ_3-oxido (Scheme 8, bottom). This transition state is ca. 9 kcal•mol^{-1} higher for **11**-Ca, consistent with the stronger Mn^{IV}–OAc bonds of **11**-Ca. The difference in reactivity between the heterometallic and homometallic clusters here shows that differences in oxidation state can affect oxygen-atom transfer chemistry indirectly by changing ancillary ligand lability, in addition to changing the nature of the oxo moiety.

With the ability to interconvert **6** and **2** by oxygen-atom transfer, a detailed mechanistic study of water incorporation into the partial cubane **6** to form cubane **2** was undertaken. Addition of water, hydroxide, and a one-electron oxidant to **6** in THF/CH_3CN mixtures afforded **2** in ca. 95% purity (Scheme 8). Removal of any single reagent either shut down production of **2** or decreased the yield substantially. The present protocol mimics the biological incorporation of an oxido ligand into the OEC and, taking into account the oxidation states, it corresponds conceptually to the putative final steps of photoactivation, the conversion of S_{-1} to S_1.

An ^{18}O labeling study was devised as a mechanistic probe that utilized the site-differentiation given by the ligand framework. Labelled base and water ($NMe_4{}^{18}OH$ and $H_2{}^{18}O$) were utilized in the water incorporation conditions. Incorporation of ^{18}O in the cubane product (**2***) was observed by ESI-MS. Although, the “bottom” oxido is missing in the partial cubane **6**, the isotopically labelled atom of **2*** could be located at any of the oxido positions in the cubane. The site of the label was interrogated by oxygen-atom transfer from **2*** to trimethylphosphine to generate **6**/**6*** and trimethylphosphine oxide. The various mechanisms of oxidative oxido incorporation into the cluster from water and oxygen-atom transfer have distinct outcomes with respect to the ratio of isotopologs of products ($^{18}OPMe_3$ vs $^{16}OPMe_3$, **6** vs **6***). Experimentally, a mixture of **6** and **6*** was observed, consistent with water incorporation and phosphine attack at one of the three top oxygens. Water is likely incorporated at the top position, although unselective incorporation cannot be ruled out, since this would also form a mixture of **6** and **6***. Nevertheless, the pathways consistent with the experimental outcome all require migration of oxido ligands within the cluster during the process of oxidative water incorporation. This provides a model compound analogue for the proposed μ-oxido migration equilibria for the OEC (Scheme 8, top).[40-41]

3.2 Effects of redox-inactive ions on cluster redox potentials

Redox-inactive ions affect electron transfer rates and potentials in small molecule monometallic complexes as well as biological and synthetic electron transfer reactions (vide supra). [106,112-113,115-116,145-147] Additionally, chemical reactions such as hydrogen- and oxygen-atom transfer, and O_2 reduction are significantly influenced by the presence of redox-inactive metals.[104,113,117,148]

Access to the two series of heterometallic manganese oxido complexes with isostructural dioxido and tetraoxido cores described in Sections 2.2 and 2.3 provide a method of probing the effect of the redox-inactive metal on the physical properties of multimetallic clusters. The ability of the framework to accommodate monocationic, dicationic, and tricationic metal ions within the same position of the clusters allows the variation of a wide range of metal properties, including ionic radius, charge, and Lewis acidity.

The potentials of the quasireversible $[Mn^{III}_2Mn^{IV}O_2]/[MMn^{III}_3O_2]$ couples of the $[MMn_3O_2]$ complexes **9** and **10** (M = Na^+, Sr^{2+}, Ca^{2+}, Zn^{2+}, and Y^{3+}) were measured using cyclic voltammetry. A significant shift of the potential was observed upon substitution of the redox-inactive metal; for example, the redox potential measured for the $[YMn_3O_2]$ cluster is 420 mV vs. the ferrocene/ferrocenium couple (Fc/Fc^+), while that of the $[SrMn_3O_2]$ compound is −70 mV vs. Fc/Fc^+, a difference of nearly 0.5 V. Although redox-inactive metals of higher charge lead to more oxidizing clusters, this shift in potential cannot be attributed to only an electrostatic effect, which was previously invoked for shifts in the reduction potential of oxo-bridged manganese dimers supported by crown ether-modified ligands with associated alkali and alkaline earth metals.[149] The potential measured for the $[ZnMn_3O_2]$ cluster is more than 200 mV more positive than that of the strontium-substituted cluster, although both contain dicationic apical metals.

When the redox potentials are plotted against the pK_a of the redox-inactive M(aqua)$^{n+}$ ion, used here as a measure of Lewis acidity, a linear dependence is observed (Figure 11), with the potential shifting by ca. 90 mV per pK_a unit. This effect likely results from the interaction of the oxido moieties with redox-inactive metals vs. manganese centers. The stronger Lewis acid draws more electron density from the oxido ligands destabilizing the higher oxidation state manganese centers and shifting the potential to more positive values. The effect of the redox-inactive metals supports previous proposals that Ca^{2+}, in addition to serving as a site for water or hydroxide coordination in the OEC, may modulate the potential of the manganese cluster for water oxidation.[26,66,150] It is important to note that the potentials of the Ca^{2+} and Sr^{2+}-substituted dioxido complexes are the same, which correlates with the observation that the OEC is active only with these two redox-inactive metals.[52,57] In other studies, the addition of redox-inactive metals has been shown to affect the rates of electron transfer involving organic or inorganic substrates.[145-146] Recently, the groups of Fukuzumi and Nam reported the rates of reduction of iron-oxo complexes to depend in a linear fashion on the Lewis acidity of redox-inactive additives.[115-116] This kinetic effect represents another consequence of association of the redox-inactive metal with transition metal oxo species.

The reduction potentials of the $[MMn_3O_4]$ cubane clusters **11**-M (M = Sr^{2+}, Ca^{2+}, Zn^{2+}, Y^{3+}, Sc^{3+}) were measured using cyclic voltammetry to determine whether a dependence on metal ion Lewis acidity could be observed for a different structural series of heterometallic manganese oxido clusters (Figure 12).[136] These complexes are also more structurally similar to the OEC and display higher oxidation state and oxido content. Again, the reduction potentials shift significantly with the nature of the fourth metal. The charge of the cation is clearly not the single influencing factor, since the Zn^{2+} species has a significantly more positive potential than the Ca^{2+} and Sr^{2+} cubanes, and the Y^{3+}, Sc^{3+}, and Mn^{3+} complexes

are all separated by more than 200 mV each. A linear correlation is observed again between the redox potentials of the $[MMn^{IV}_3O_4]/[MMn^{III}Mn^{IV}_2O_4]$ couple and the Lewis acidity of the redox-inactive metal M (Figure 11). With the inclusion of the potential of the $[Mn^{III}Mn^{IV}_3O_4]/[Mn^{III}_2Mn^{IV}_2O_4]$ couple, measured from cyclic voltammetry of **2**, the redox potentials of the structurally similar $[MMn_3O_4]$ clusters (M = Sr^{2+}, Ca^{2+}, Zn^{2+} Y^{3+}, Sc^{3+}, Mn^{3+}) span over 1.2 V, corresponding to a 28 kcal/mol change in energy. This large difference in redox potential, effected by simple substitution, is consistent with observations that the addition of Lewis acids to both inorganic and organic compounds can have a large effect on reactivity and kinetic properties.[104,113-117,145-146,148]

The $SrMn_3O_4$ and $CaMn_3O_4$ have very similar reduction potentials, analogous to the MMn_3O_2 species. Borovik's Ca-(μ-OH)-M and Sr-(μ-OH)-M complexes have similar potentials as well.[106] Given the expected large effect on the cluster potential by other metals (Figure 11), these results suggest that Sr^{2+} restores partial activity in Ca-depleted PSII because the potentials of the resulting clusters are similar. The difference in catalytic activity between the Ca^{2+} and Sr^{2+} OEC may be caused by other subtle effects, such as different levels of activation of a coordinated water substrate for O–O bond formation.

Although the $[MMn_3O_4]$ and $[MMn_3O_2]$ clusters differ significantly in oxidation state, geometry, and coordination mode of the ligand framework, the linear correlations between redox potential and Lewis acidity of both series of compounds have the same slope (Figure 11). This observation suggests that the dependence of reduction potential on Lewis acidity may be a general phenomenon for mixed metal oxide clusters. Notably, the intercepts of the two lines differ by ca. 900 mV with the $[MMn^{IV}_3O_4]$ complexes having more negative reduction potentials than the corresponding $[MMn^{IV}Mn^{III}_2O_2]$ despite the lower oxidation state of the dioxide species. This large difference in potential is likely due to the lower oxide content in compounds **9** vs. **11**, pointing to a different path of tuning the cluster potential by varying the number of oxide moieties. The synthetic $CaMn_3$ clusters ($[CaMn^{IV}_3O_4]$ and $[CaMn^{III}_2Mn^{IV}O_2]$) have potentials negative of the thermodynamic potential for water oxidation, probably due to a combination of the higher oxidation state, different Mn/O ratio, and the nature of the ancillary ligands for the OEC ("$CaMn^{IV}_3Mn^{V}O_5$", for simplicity).

Beyond insights related to the OEC, the systematic effects observed for redox-inactive metals in clusters of different structures suggest that the redox chemistry of other materials could be tuned quantitatively based on the same approach. For isostructural catalytic sites the reduction potential could be affected by the simple replacement of the redox-inactive metal toward lowering overpotentials or making a reaction thermodynamically favorable. The same principles may be applicable to larger clusters or other materials with strong direct or indirect interactions between different metals. In the context of mixed metal oxides, for example, applications include water oxidation and dioxygen reduction catalysis and battery materials.[15-16,20-23]

4. Conclusions and Outlook

A synthetic methodology with unprecedented structural control was developed for the synthesis of manganese oxido complexes that model the oxygen-evolving complex of PSII and proposed sites of catalysis in mixed metal oxide catalysts for water oxidation. A stepwise oxidative functionalization strategy was employed by the controlled addition of metal source and oxidant to a trimanganese(II) complex supported by a rigid multinucleating framework. Tetramanganese clusters of varying oxide content, as well as heterometallic tetranuclear clusters containing different redox-inactive metals were isolated in several oxidation states. These structural models have provided insight related to the properties and function of the OEC. The site-differentiation of the metals in these clusters have allowed for

isotopic labeling studies to support pathways of oxide migration within the cluster, reminiscent of proposals for the OEC. Electrochemical studies of isostructural series of manganese dioxido and tetraoxido clusters revealed a linear dependence of the redox potentials of the clusters on the Lewis acidity of the incorporated redox-inactive metal. The effect of the Lewis acidity of redox-inactive metal is remarkably high, shifting the potential over a range of more than 1 V. These results point to a role of Ca^{2+} in PSII for tuning the reduction potential of the catalytic site. Additionally, the effects discovered in these studies may be applicable to a variety of catalytic and functional materials with discrete or extended structure.

Future work includes the synthesis of models of the full OEC by functionalizing the $[CaMn_3O_4]$ cubane with a fourth manganese center for greater similarity to the structure of the biological $[CaMn_4O_5]$ cluster. Spectroscopic studies are ongoing to complement investigations of the biological system and to provide insight into the electronic structure of these compounds. Related heterometallic complexes of other transition metals supported by this and other ligand frameworks are of interest to test the generality of the reactivity and electrochemical studies beyond manganese. Additionally, the study of mixed transition metal oxide clusters is an exciting area given the interesting properties emerging for heterogeneous metal oxides applied to water oxidation and oxygen reduction catalysis, and to metal oxide battery materials. These studies are expected to afford a detailed understanding of the effect of cluster structure on reactivity related to O_2 chemistry in the biological and artificial systems: electron transfer chemistry, oxygen-atom transfer, and ultimately O–O bond formation and cleavage. The synthetic methodologies described here are hoped to provide a stimulating precedent for the rational design and study of other complex clusters of practical and fundamental interest.

Acknowledgments

We thank California Institute of Technology, the Searle Scholars Program, NSF CAREER CHE-1151918, NIH R01 GM102687A (T.A.), a Sandia Campus Executive Fellowship (E.Y.T.), and NSF Graduate Fellowships (E.Y.T. and J.S.K.) for financial support. We are grateful to collaborators for insightful discussions, and to colleagues and coworkers for a stimulating environment to do science at Caltech.

REFERENCES

(1). Wydrzynski, TJ.; Satoh, K. Photosystem II: The Light-Driven Water: Plastoquinone Oxidoreductase. Vol. Vol. 22. Springer; Dordrecht, The Netherlands: 2005.

(2). McEvoy JP, Brudvig GW. Chem. Rev. 2006; 106:4455. [PubMed: 17091926]

(3). Brudvig GW. Philos. Trans. R. Soc. B-Biol. Sci. 2008; 363:1211.

(4). Joliot P, Barbieri G, Chabaud R. Photochem Photobiol. 1969; 10:309.

(5). Kok B, Forbush B, Mcgloin M. Photochem Photobiol. 1970; 11:457. [PubMed: 5456273]

(6). Symes MD, Surendranath Y, Lutterman DA, Nocera DG. J. Am. Chem. Soc. 2011; 133:5174. [PubMed: 21413703]

(7). Risch M, Klingan K, Ringleb F, Chernev P, Zaharieva I, Fischer A, Dau H. ChemSusChem. 2012; 5:542. [PubMed: 22323319]

(8). Zaharieva I, Najafpour MM, Wiechen M, Haumann M, Kurz P, Dau H. Energy Environ. Sci. 2011; 4:2400.

(9). Wiechen M, Zaharieva I, Dau H, Kurz P. Chem. Sci. 2012

(10). Zaharieva I, Chernev P, Risch M, Klingan K, Kohlhoff M, Fischer A, Dau H. Energy Environ. Sci. 2012; 5:7081.

(11). Najafpour MM, Ehrenberg T, Wiechen M, Kurz P. Angew. Chem. Int. Ed. 2010; 49:2233.

(12). Najafpour MM, Nayeri S, Pashaei B. Dalton Trans. 2011; 40:9374. [PubMed: 21850343]

(13). Shevela D, Koroidov S, Najafpour MM, Messinger J, Kurz P. Chem. Eur. J. 2011; 17:5415. [PubMed: 21465582]

(14). Najafpour MM, Pashaei B, Nayeri S. Dalton Trans. 2012; 41:4799. [PubMed: 22382465]

(15). Suntivich J, May KJ, Gasteiger HA, Goodenough JB, Shao-Horn Y. Science. 2011; 334:1383. [PubMed: 22033519]

(16). Smith RDL, Prévot MS, Fagan RD, Zhang Z, Sedach PA, Siu MKJ, Trudel S, Berlinguette CP. Science. 2013; 340:60. [PubMed: 23539180]

(17). Liang Y, Wang H, Zhou J, Li Y, Wang J, Regier T, Dai H. J. Am. Chem. Soc. 2012; 134:3517. [PubMed: 22280461]

(18). Suntivich J, Gasteiger HA, Yabuuchi N, Nakanishi H, Goodenough JB, Shao-Horn Y. Nat. Chem. 2011; 3:546. [PubMed: 21697876]

(19). Hamdani M, Singh RN, Chartier P. Int. J. Electrochem. Sci. 2010; 5:556.

(20). Goodenough JB, Kim Y. Chem. Mater. 2009; 22:587.

(21). Whittingham MS. Chem. Rev. 2004; 104:4271. [PubMed: 15669156]

(22). Reddy MV, Subba Rao GV, Chowdari BVR. Chem. Rev. 2013; 113:5364. [PubMed: 23548181]

(23). Melot BC, Tarascon JM. Acc. Chem. Res. 2013; 46:1226. [PubMed: 23282038]

(24). Kirby JA, Robertson AS, Smith JP, Thompson AC, Cooper SR, Klein MP. J. Am. Chem. Soc. 1981; 103:5529.

(25). Kirby JA, Goodin DB, Wydrzynski T, Robertson AS, Klein MP. J. Am. Chem. Soc. 1981; 103:5537.

(26). Yachandra VK, Sauer K, Klein MP. Chem. Rev. 1996; 96:2927. [PubMed: 11848846]

(27). Sauer K, Yano J, Yachandra V. Photosynth Res. 2005; 85:73. [PubMed: 15977060]

(28). Yano J, Kern J, Sauer K, Latimer MJ, Pushkar Y, Biesiadka J, Loll B, Saenger W, Messinger J, Zouni A, Yachandra VK. Science. 2006; 314:821. [PubMed: 17082458]

(29). Messinger J, Nugent JHA, Evans MCW. Biochemistry. 1997; 36:11055. [PubMed: 9333322]

(30). Messinger J, Robblee JH, Yu WO, Sauer K, Yachandra VK, Klein MP. J. Am. Chem. Soc. 1997; 119:11349.

(31). Peloquin JM, Campbell KA, Randall DW, Evanchik MA, Pecoraro VL, Armstrong WH, Britt RD. J. Am. Chem. Soc. 2000; 122:10926.

(32). Dismukes GC, Siderer Y. FEBS Letters. 1980; 121:78.

(33). Dismukes GC, Siderer Y. P Natl Acad Sci-Biol. 1981; 78:274.

(34). Dismukes GC, Ferris K, Watnick P. Photobioch Photobiop. 1982; 3:243.

(35). Ferreira KN, Iverson TM, Maghlaoui K, Barber J, Iwata S. Science. 2004; 303:1831. [PubMed: 14764885]

(36). Umena Y, Kawakami K, Shen JR, Kamiya N. Nature. 2011; 473:55. [PubMed: 21499260]

(37). Luber S, Rivalta I, Umena Y, Kawakami K, Shen J-R, Kamiya N, Brudvig GW, Batista VS. Biochemistry. 2011; 50:6308. [PubMed: 21678908]

(38). Ames W, Pantazis DA, Krewald V, Cox N, Messinger J, Lubitz W, Neese F. J. Am. Chem. Soc. 2011; 133:19743. [PubMed: 22092013]

(39). Yano J, Kern J, Irrgang K-D, Latimer MJ, Bergmann U, Glatzel P, Pushkar Y, Biesiadka J, Loll B, Sauer K, Messinger J, Zouni A, Yachandra VK. Proc. Natl. Acad. Sci. USA. 2005; 102:12047. [PubMed: 16103362]

(40). Kusunoki M. J. Photochem. Photobiol. B. 2011; 104:100. [PubMed: 21592813]

(41). Pantazis DA, Ames W, Cox N, Lubitz W, Neese F. Angew. Chem. Int. Ed. 2012; 51:9935.

(42). Siegbahn PEM. Chem. Eur. J. 2008; 14:8290. [PubMed: 18680116]

(43). Grundmeier A, Dau H. Biochim. Biophys. Acta - Bioenergetics. 2012; 1817:88.

(44). Messinger J, Badger M, Wydrzynski T. Proc. Natl. Acad. Sci. USA. 1995; 92:3209. [PubMed: 11607525]

(45). Hillier W, Messinger J, Wydrzynski T. Biochemistry. 1998; 37:16908. [PubMed: 9836583]

(46). Rapatskiy L, Cox N, Savitsky A, Ames WM, Sander J, Nowaczyk MM, Rögner M, Boussac A, Neese F, Messinger J, Lubitz W. J. Am. Chem. Soc. 2012; 134:16619. [PubMed: 22937979]

(47). Dasgupta J, van Willigen RT, Dismukes GC. Phys. Chem. Chem. Phys. 2004; 6:4793.
(48). Vincent JB, Christou G. Inorg. Chim. Acta. 1987; 136:L41.
(49). Brudvig GW, Crabtree RH. Proc. Natl. Acad. Sci. USA. 1986; 83:4586. [PubMed: 3460059]
(50). Pecoraro VL, Baldwin MJ, Caudle MT, Hsieh WY, Law NA. Pure Appl. Chem. 1998; 70:925.
(51). Vrettos JS, Limburg J, Brudvig GW. Biochim. Biophys. Acta - Bioenergetics. 2001; 1503:229.
(52). Vrettos JS, Stone DA, Brudvig GW. Biochemistry. 2001; 40:7937. [PubMed: 11425322]
(53). Siegbahn PEM, Crabtree RH. J. Am. Chem. Soc. 1999; 121:117.
(54). Siegbahn PEM. Philos. Trans. R. Soc. B-Biol. Sci. 2008; 363:1221.
(55). Sproviero EM, Gascón JA, McEvoy JP, Brudvig GW, Batista VS. J. Am. Chem. Soc. 2008; 130:3428. [PubMed: 18290643]
(56). Siegbahn PEM. Acc. Chem. Res. 2009; 42:1871. [PubMed: 19856959]
(57). Ghanotakis DF, Babcock GT, Yocum CF. FEBS Letters. 1984; 167:127.
(58). Boussac A, Zimmermann JL, Rutherford AW. Biochemistry. 1989; 28:8984. [PubMed: 2557913]
(59). Yocum CF. Biochim. Biophys. Acta - Bioenergetics. 1991; 1059:1.
(60). Yocum CF. Coord. Chem. Rev. 2008; 252:296.
(61). Boussac A, Rutherford AW. Biochemistry. 1988; 27:3476.
(62). Pushkar Y, Yano J, Sauer K, Boussac A, Yachandra VK. Proc. Natl. Acad. Sci. USA. 2008; 105:1879. [PubMed: 18250316]
(63). Cox N, Rapatskiy L, Su J-H, Pantazis DA, Sugiura M, Kulik L, Dorlet P, Rutherford AW, Neese F, Boussac A, Lubitz W, Messinger J. J. Am. Chem. Soc. 2011; 133:3635. [PubMed: 21341708]
(64). Lee C-I, Lakshmi KV, Brudvig GW. Biochemistry. 2007; 46:3211. [PubMed: 17309233]
(65). Yachandra VK, Yano J. J. Photochem. Photobiol. B. 2011; 104:51. [PubMed: 21524917]
(66). Riggs-Gelasco PJ, Mei R, Ghanotakis DF, Yocum CF, Penner-Hahn JE. J. Am. Chem. Soc. 1996; 118:2400.
(67). Lohmiller T, Cox N, Su J-H, Messinger J, Lubitz W. J. Biol. Chem. 2012; 287:24721. [PubMed: 22549771]
(68). Kanan MW, Yano J, Surendranath Y, Dincă M, Yachandra VK, Nocera DG. J. Am. Chem. Soc. 2010; 132:13692. [PubMed: 20839862]
(69). Wieghardt K. Angew. Chem. Int. Ed. Engl. 1989; 28:1153.
(70). Cady CW, Crabtree RH, Brudvig GW. Coord. Chem. Rev. 2008; 252:444. [PubMed: 21037800]
(71). Sproviero EM, Gascón JA, McEvoy JP, Brudvig GW, Batista VS. Coord. Chem. Rev. 2008; 252:395. [PubMed: 19190716]
(72). Christou G. Acc. Chem. Res. 1989; 22:328.
(73). Pecoraro VL, Baldwin MJ, Gelasco A. Chem. Rev. 1994; 94:807.
(74). Manchanda R, Brudvig GW, Crabtree RH. Coord. Chem. Rev. 1995; 144:1.
(75). Yagi M, Kaneko M. Chem. Rev. 2000; 101:21. [PubMed: 11712192]
(76). Mukhopadhyay S, Mandal SK, Bhaduri S, Armstrong WH. Chem. Rev. 2004; 104:3981. [PubMed: 15352784]
(77). Wu AJ, Penner-Hahn JE, Pecoraro VL. Chem. Rev. 2004; 104:903. [PubMed: 14871145]
(78). Mullins CS, Pecoraro VL. Coord. Chem. Rev. 2008; 252:416. [PubMed: 19081816]
(79). Plaksin PM, Stoufer RC, Mathew M, Palenik GJ. J. Am. Chem. Soc. 1972; 94:2121.
(80). Cooper SR, Calvin M. J. Am. Chem. Soc. 1977; 99:6623.
(81). Cooper SR, Dismukes GC, Klein MP, Calvin M. J. Am. Chem. Soc. 1978; 100:7248.
(82). Kirby JA, Robertson AS, Smith JP, Thompson AC, Cooper SR, Klein MP. J. Am. Chem. Soc. 1981; 103:5529.
(83). Dismukes GC, Siderer Y. Proc. Natl. Acad. Sci. USA. 1981; 78:274. [PubMed: 16592949]
(84). Guiles RD, Zimmermann JL, McDermott AE, Yachandra VK, Cole JL, Dexheimer SL, Britt RD, Wieghardt K, Bossek U. Biochemistry. 1990; 29:471. [PubMed: 2154247]
(85). Chan MK, Armstrong WH. J. Am. Chem. Soc. 1991; 113:5055.

(86). Chen H, Faller JW, Crabtree RH, Brudvig GW. J. Am. Chem. Soc. 2004; 126:7345. [PubMed: 15186173]

(87). Philouze C, Blondin G, Girerd J-J, Guilhem J, Pascard C, Lexa D. J. Am. Chem. Soc. 1994; 116:8557.

(88). Limburg J, Brudvig GW, Crabtree RH. J. Am. Chem. Soc. 1997; 119:2761.

(89). Limburg J, Vrettos JS, Liable-Sands LM, Rheingold AL, Crabtree RH, Brudvig GW. Science. 1999; 283:1524. [PubMed: 10066173]

(90). Limburg J, Vrettos JS, Chen H, de Paula JC, Crabtree RH, Brudvig GW. J. Am. Chem. Soc. 2000; 123:423. [PubMed: 11456544]

(91). Vincent JB, Christmas C, Chang HR, Li Q, Boyd PDW, Huffman JC, Hendrickson DN, Christou G. J. Am. Chem. Soc. 1989; 111:2086.

(92). Vincent JB, Christmas C, Huffman JC, Christou G, Chang H-R, Hendrickson DN. J. Chem. Soc., Chem. Commun. 1987:236. 0.

(93). Li Q, Vincent JB, Libby E, Chang H-R, Huffman JC, Boyd PDW, Christou G, Hendrickson DN. Angew. Chem. Int. Ed. Engl. 1988; 27:1731.

(94). Ruettinger WF, Campana C, Dismukes GC. J. Am. Chem. Soc. 1997; 119:6670.

(95). Dismukes GC, Brimblecombe R, Felton GAN, Pryadun RS, Sheats JE, Spiccia L, Swiegers GF. Acc. Chem. Res. 2009; 42:1935. [PubMed: 19908827]

(96). Brimblecombe R, Swiegers GF, Dismukes GC, Spiccia L. Angew. Chem. Int. Ed. 2008; 47:7335.

(97). Hocking RK, Brimblecombe R, Chang L-Y, Singh A, Cheah MH, Glover C, Casey WH, Spiccia L. Nat. Chem. 2011; 3:461. [PubMed: 21602861]

(98). Wieghardt K, Bossek U, Gebert W. Angew. Chem. Int. Ed. Engl. 1983; 22:328.

(99). Dubé CE, Wright DW, Pal S, Bonitatebus PJ Jr. Armstrong WH. J. Am. Chem. Soc. 1998; 120:3704.

(100). Mishra A, Wernsdorfer W, Abboud KA, Christou G. Chem. Commun. 2005:54.

(101). Mishra A, Yano J, Pushkar Y, Yachandra VK, Abboud KA, Christou G. Chem. Commun. 2007:1538.

(102). Hewitt IJ, Tang J-K, Madhu NT, Clerac R, Buth G, Anson CE, Powell AK. Chem. Commun. 2006:2650.

(103). Nayak S, Nayek HP, Dehnen S, Powell AK, Reedijk J. Dalton Trans. 2011; 40:2699. [PubMed: 21327234]

(104). Park YJ, Ziller JW, Borovik AS. J. Am. Chem. Soc. 2011; 133:9258. [PubMed: 21595481]

(105). Mukherjee S, Stull JA, Yano J, Stamatatos TC, Pringouri K, Stich TA, Abboud KA, Britt RD, Yachandra VK, Christou G. Proc. Natl. Acad. Sci. USA. 2012; 109:2257. [PubMed: 22308383]

(106). Park YJ, Cook SA, Sickerman NS, Sano Y, Ziller JW, Borovik AS. Chem. Sci. 2013; 4:717. [PubMed: 24058726]

(107). Mishra A, Pushkar Y, Yano J, Yachandra VK, Wernsdorfer W, Abboud KA, Christou G. Inorg. Chem. 2008; 47:1940. [PubMed: 18281933]

(108). Kotzabasaki V, Siczek M, Lis T, Milios CJ. Inorg. Chem. Commun. 2011; 14:213.

(109). Koumousi ES, Mukherjee S, Beavers CM, Teat SJ, Christou G, Stamatatos TC. Chem. Commun. 2011; 47:11128.

(110). Jerzykiewicz LB, Utko J, Duczmal M, Sobota P. Dalton Trans. 2007:825. [PubMed: 17297508]

(111). Li N, Wang M, Ma C-B, Hu M-Q, Zhou R-W, Chen H, Chen C-N. Inorg. Chem. Commun. 2010; 13:730.

(112). Lacy DC, Park YJ, Ziller JW, Yano J, Borovik AS. J. Am. Chem. Soc. 2012; 134:17526. [PubMed: 22998407]

(113). Chen J, Lee Y-M, Davis KM, Wu X, Seo MS, Cho K-B, Yoon H, Park YJ, Fukuzumi S, Pushkar YN, Nam W. J. Am. Chem. Soc. 2013; 135:6388. [PubMed: 23324100]

(114). Yoon H, Lee Y-M, Wu X, Cho K-B, Sarangi R, Nam W, Fukuzumi S. J. Am. Chem. Soc. 2013; 135:9186. [PubMed: 23742163]

(115). Fukuzumi S, Morimoto Y, Kotani H, Naumov P, Lee YM, Nam W. Nat. Chem. 2010; 2:756. [PubMed: 20729896]

(116). Morimoto Y, Kotani H, Park J, Lee YM, Nam W, Fukuzumi S. J. Am. Chem. Soc. 2011; 133:403. [PubMed: 21158434]

(117). Leeladee P, Baglia RA, Prokop KA, Latifi R, de Visser SP, Goldberg DP. J. Am. Chem. Soc. 2012; 134:10397. [PubMed: 22667991]

(118). Stack TDP, Holm RH. J. Am. Chem. Soc. 1987; 109:2546.

(119). Venkateswara Rao P, Holm RH. Chem. Rev. 2003; 104:527. [PubMed: 14871134]

(120). Stack TDP, Holm RH. J. Am. Chem. Soc. 1988; 110:2484.

(121). Ciurli S, Carrie M, Weigel JA, Carney MJ, Stack TDP, Papaefthymiou GC, Holm RH. J. Am. Chem. Soc. 1990; 112:2654.

(122). Zhou J, Raebiger JW, Crawford CA, Holm RH. J. Am. Chem. Soc. 1997; 119:6242.

(123). Stamatatos TC, Efthymiou CG, Stoumpos CC, Perlepes SP. Eur. J. Inorg. Chem. 2009; 2009:3361.

(124). Tsui EY, Day MW, Agapie T. Angew. Chem. Int. Ed. 2011; 50:1668.

(125). Tsui EY, Kanady JS, Day MW, Agapie T. Chem. Commun. 2011; 47:4189.

(126). Kanady JS, Tsui EY, Day MW, Agapie T. Science. 2011; 333:733. [PubMed: 21817047]

(127). Wang S, Huffman JC, Folting K, Streib WE, Lobkovsky EB, Christou G. Angew. Chem. Int. Ed. Engl. 1991; 30:1672.

(128). Wang S, Tsai H-L, Hagen KS, Hendrickson DN, Christou G. J. Am. Chem. Soc. 1994; 116:8376.

(129). Aubin SMJ, Wemple MW, Adams DM, Tsai H-L, Christou G, Hendrickson DN. J. Am. Chem. Soc. 1996; 118:7746.

(130). Aromi G, Wemple MW, Aubin SJ, Folting K, Hendrickson DN, Christou G. J. Am. Chem. Soc. 1998; 120:5850.

(131). Aliaga-Alcalde N, Edwards RS, Hill SO, Wernsdorfer W, Folting K, Christou G. J. Am. Chem. Soc. 2004; 126:12503. [PubMed: 15453784]

(132). Kanady JS, Tran R, Stull JA, Lu L, Stich TA, Day MW, Yano J, Britt RD, Agapie T. Chem. Sci. 2013

(133). Caudle MT, Pecoraro VL. J. Am. Chem. Soc. 1997; 119:3415.

(134). Tsui EY, Tran R, Yano J, Agapie T. Nat. Chem. 2013; 5:293. [PubMed: 23511417]

(135). Kanady JS, Mendoza-Cortes JL, Tsui EY, Nielsen RJ, Goddard WA, Agapie T. J. Am. Chem. Soc. 2013; 135:1073. [PubMed: 23241061]

(136). Tsui EY, Agapie T. Proc. Natl. Acad. Sci. USA. 2013; 110:10084. [PubMed: 23744039]

(137). Cheniae GM, Martin IF. Biochem Bioph Res Co. 1967; 28:89.

(138). Siegbahn PEM. Phys. Chem. Chem. Phys. 2012; 14:4849. [PubMed: 22278436]

(139). Hillier W, Wydrzynski T. Phys. Chem. Chem. Phys. 2004; 6:4882.

(140). Tagore R, Chen, Crabtree RH, Brudvig GW. J. Am. Chem. Soc. 2006; 128:9457. [PubMed: 16848483]

(141). Tagore R, Crabtree RH, Brudvig GW. Inorg. Chem. 2007; 46:2193. [PubMed: 17295472]

(142). Ohlin CA, Brimblecombe R, Spiccia L, Casey WH. Dalton Trans. 2009:5278. 0. [PubMed: 19565077]

(143). Pecoraro, VL.; Hsieh, WY. Manganese and Its Role in Biological Systems. Sigel, A.; Sigel, H., editors. Vol. Vol. 37. Marcel Dekker, Inc.; New York: 2000. p. 429

(144). Siegbahn PEM. J. Am. Chem. Soc. 2013; 135:9442. [PubMed: 23742698]

(145). Fukuzumi, S. Progress in Inorganic Chemistry. Karlin, KD., editor. Vol. Vol. 56. John Wiley & Sons Inc; New York: 2009. p. 49

(146). Fukuzumi S, Ohkubo K. Coord. Chem. Rev. 2010; 254:372.

(147). Fukuzumi S, Ohkubo K. Chem. Eur. J. 2000; 6:4532. [PubMed: 11192086]

(148). Park J, Morimoto Y, Lee YM, Nam W, Fukuzumi S. J. Am. Chem. Soc. 2011; 133:5236. [PubMed: 21410258]

(149). Horwitz CP, Ciringh Y. Inorg. Chim. Acta. 1994; 225:191.

(150). Haumann M, Junge W. Biochim. Biophys. Acta - Bioenergetics. 1999; 1411:121.

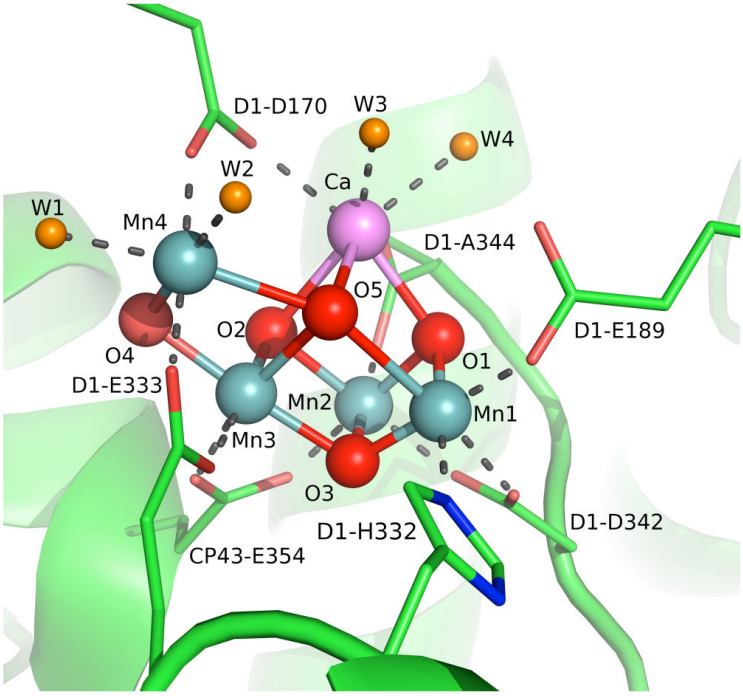

Figure 1.
Structure of OEC from single crystal X-ray diffraction studies.[36]

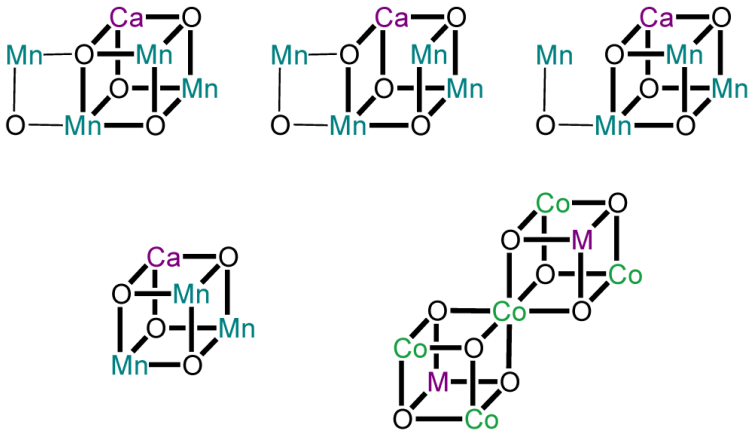

Figure 2.

Proposed structure of the OEC from single crystal XRD studies (top left)[35-36] and more open structures proposed from XAS and computational studies (top middle, right).[40-41] Proposed structure of catalytic sites in calcium manganese oxide water oxidation catalysts (bottom left)[8-9] and of cobalt oxide water oxidation catalysts (bottom right).[6]

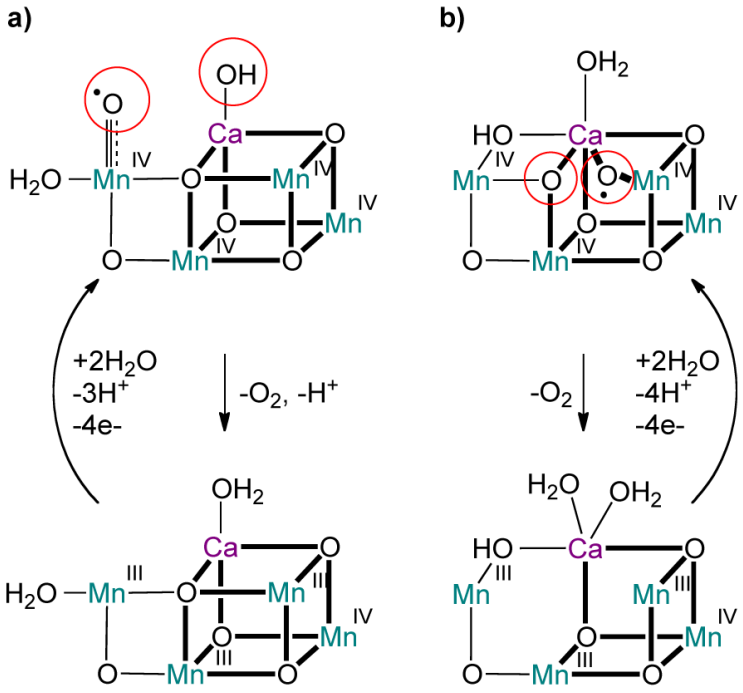

Figure 3.

Recent proposed mechanisms of O–O bond formation in the OEC,[50,55-56] with sites of substrate incorporation highlighted in red.

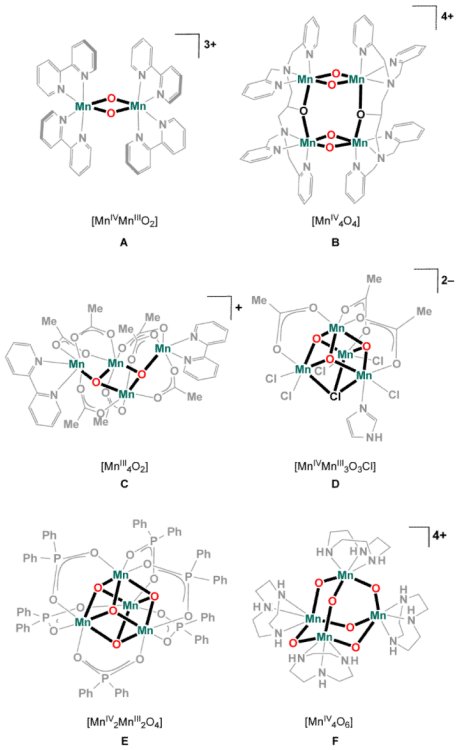

Figure 4.
Selected examples of di- and tetramanganese oxido clusters.[79,85,92-94,98]

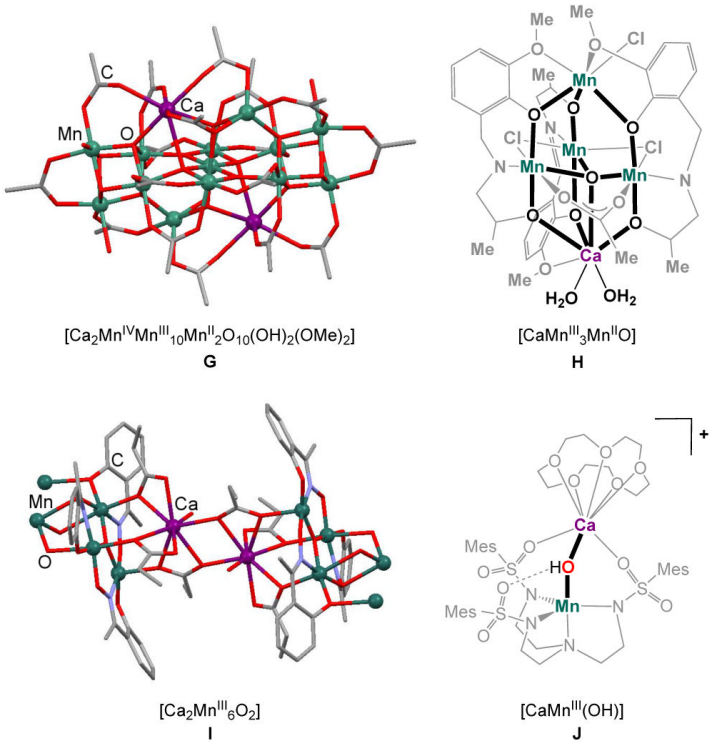

Figure 5.
Structurally characterized heterometallic calcium-manganese clusters with bridging oxide or hydroxide moieties.[100,102,104,108]

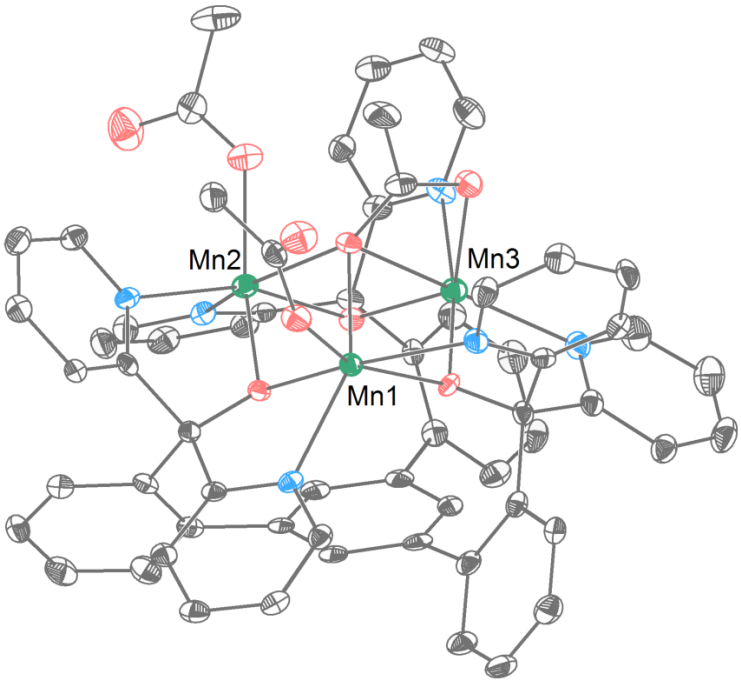

Figure 6.
Solid-state structure of **1**.

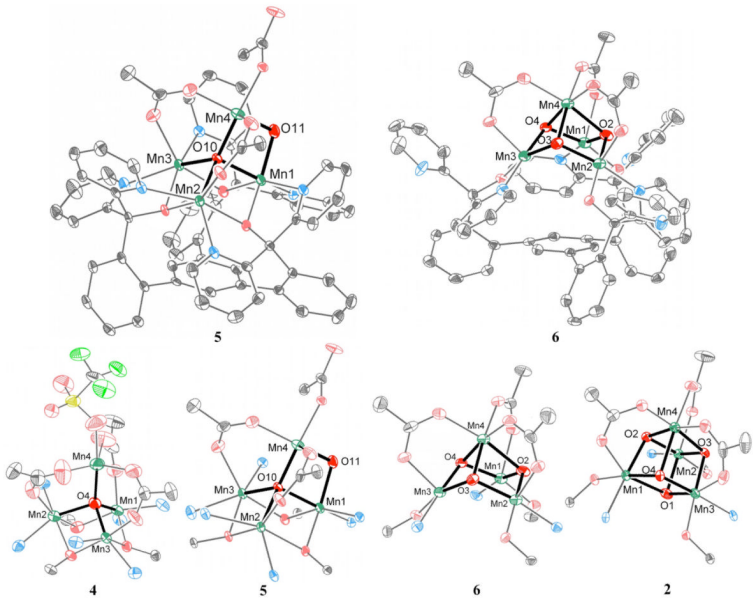

Figure 7.
Solid-state structures of tetramanganese complexes **2**-**6**.

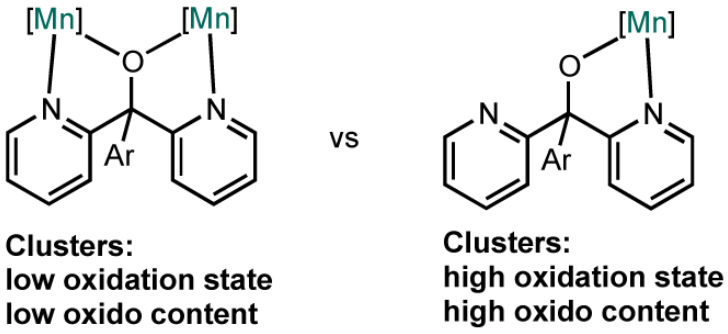

Figure 8.
Ligand flexibility as function of cluster oxido content and oxidation state: binding modes of dipyridylalkoxide arms.

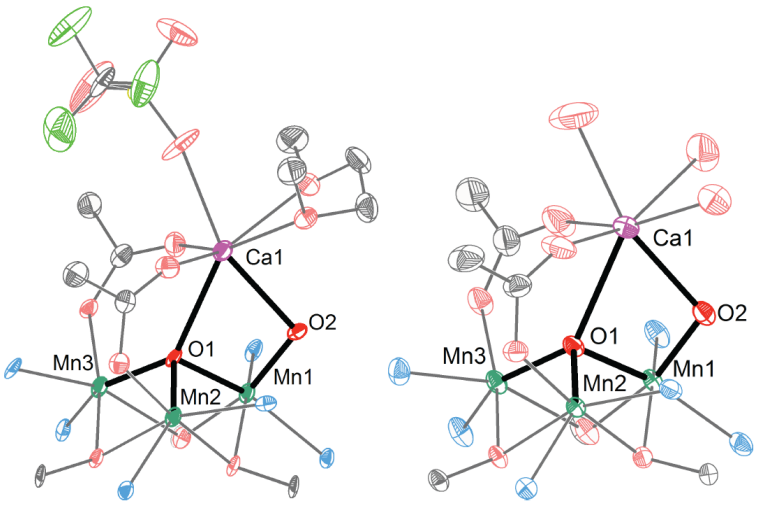

Figure 9.
Truncated solid-state structures of [**9**-Ca(DME)(OTf)]$^{2+}$ and [**9**-Ca$(OH_2)_3$]$^{3+}$.

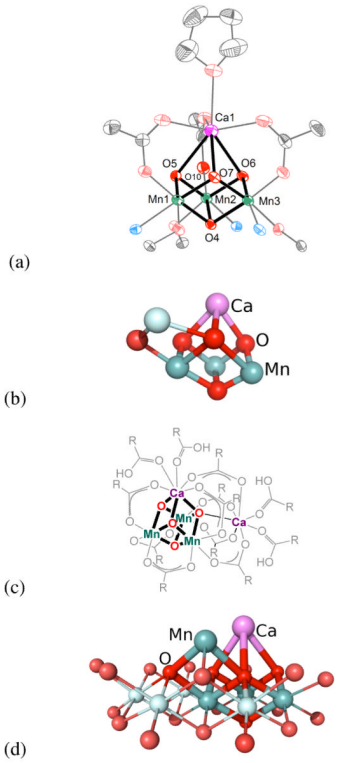

Figure 10.

Comparison of $[CaMn_3O_4]$ structures. (a) Truncated view of the solid-state structure of **11**-Ca. (b) $CaMn_4O_5$ cluster of the OEC as found in the 1.9 Å-resolution structure,[36] with the $[CaMn_3O_4]$ subsite emphasized by thicker bonds. (c) $[Ca_2Mn_3O_4]$ cluster supported by pivalate ligands, with the $[CaMn_3O_4]$ subsite emphasized by bold bonds.[105] (d) Schematic drawing of one proposed structure of calcium-doped manganese oxide materials.[9]

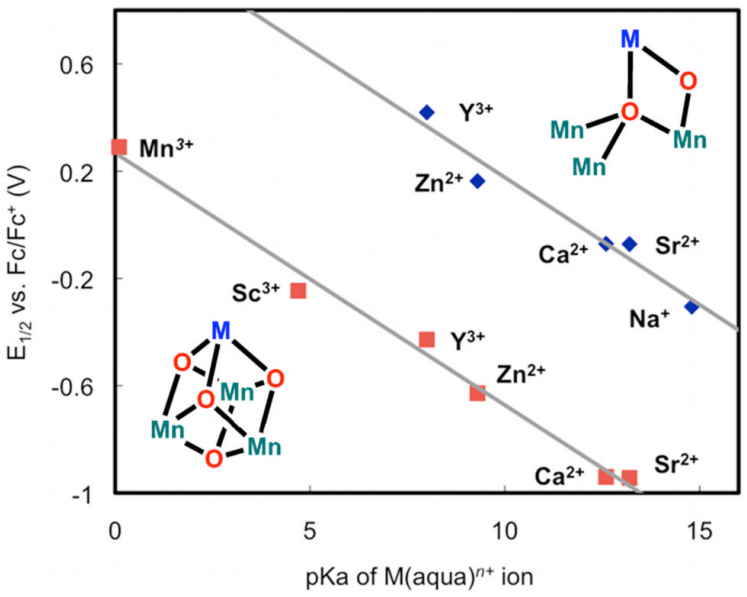

Figure 11.

Redox potentials of heterometallic trimanganese tetraoxido (red squares) and dioxido (blue diamonds) clusters plotted against the pK_a of the corresponding metal(aqua)$^{n+}$ ion, used as a measure of Lewis acidity.[136] Figure reproduced from ref. 136.

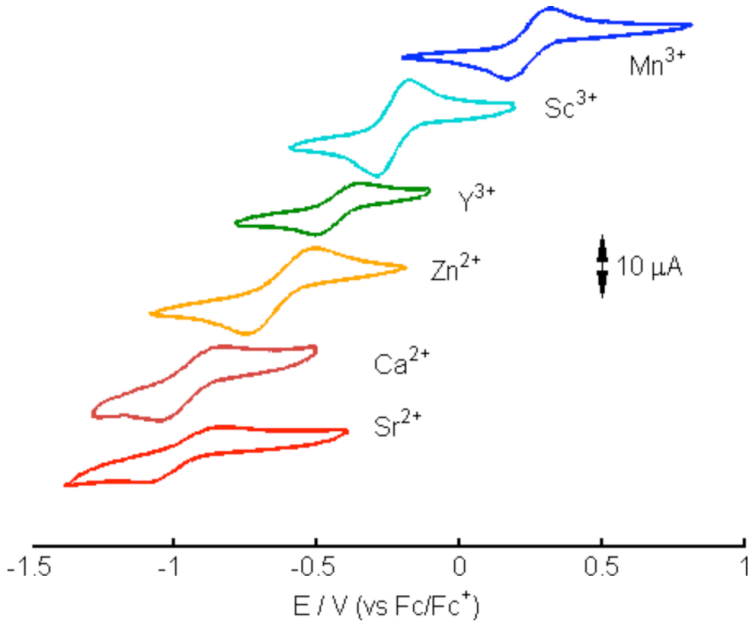

Figure 12.
Cyclic voltammograms of the $[MMn^{IV}_3O_4]/[MMn^{III}Mn^{IV}_2O_4]$ couples of *N*,*N*-dimethylacetamide solutions of MMn_3O_4 complexes at a scan rate of 100 mV/s. Potentials are referenced to the ferrocene/ferrocenium couple. Figure reproduced from ref. 136.

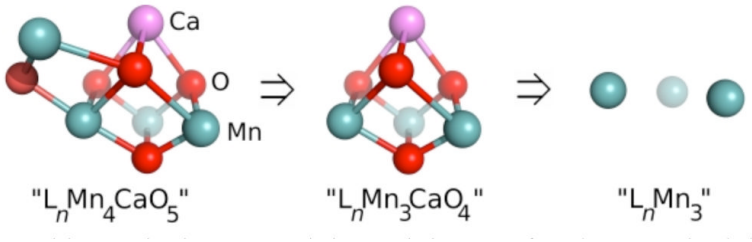

Scheme 1.
Retrosynthetic analysis for the synthesis of an OEC model.

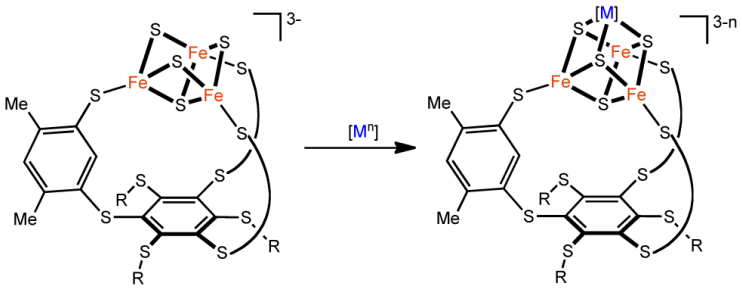

Scheme 2.
Metal incorporation into subsite-differentiated Fe_3MS_4 clusters.[122]

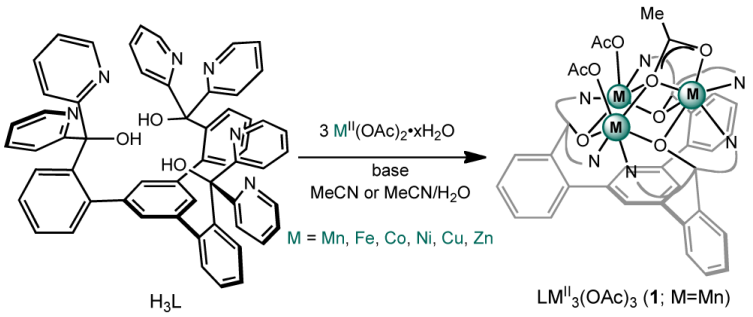

Scheme 3.
Synthesis of trimetallic complexes $LM^{II}_3(OAc)_3$ (**1**; M = Mn).

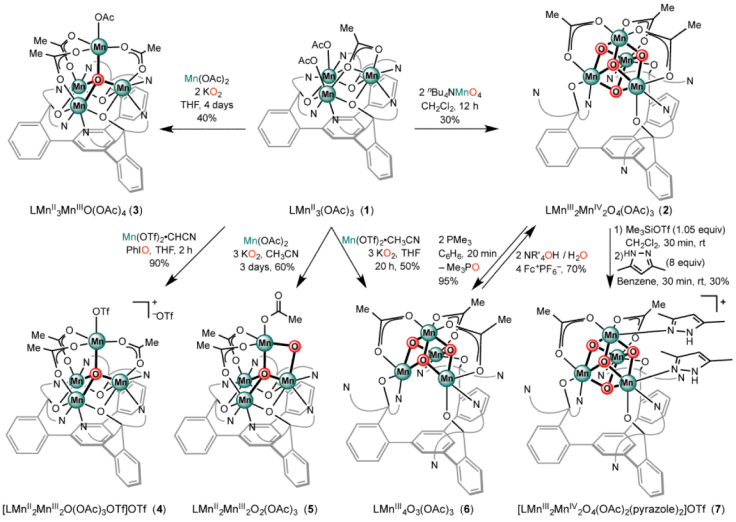

Scheme 4.

Synthesis and interconversion of tetramanganese complexes **2-7**.

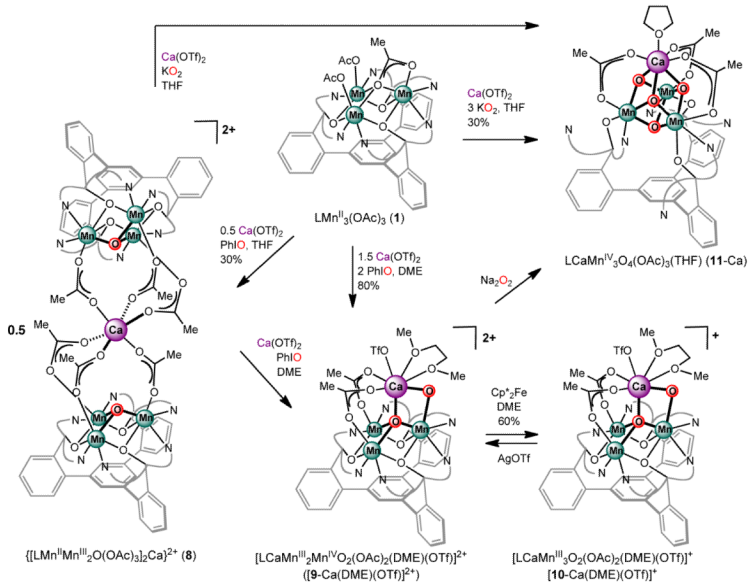

Scheme 5.
Synthesis of $CaMn_3O_x$ clusters.

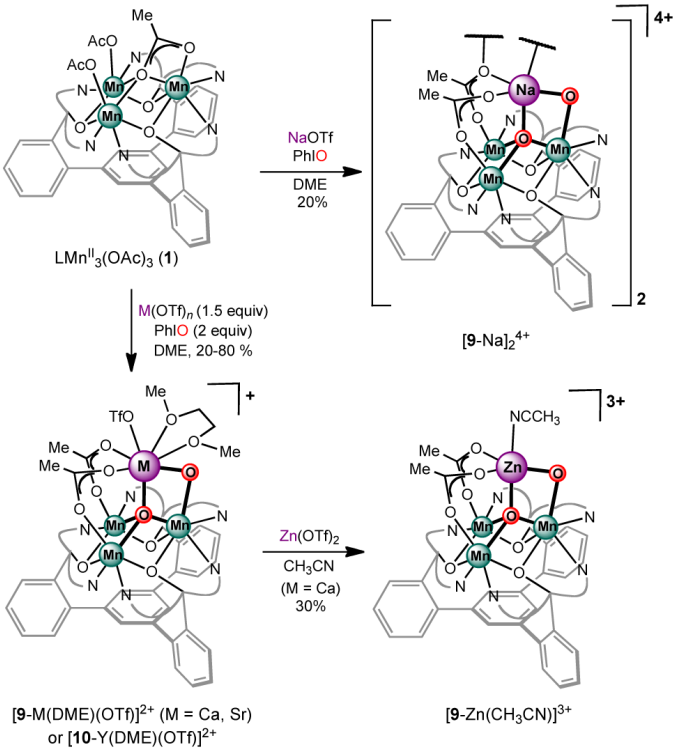

Scheme 6.
Synthesis of heterometallic dioxido complexes.

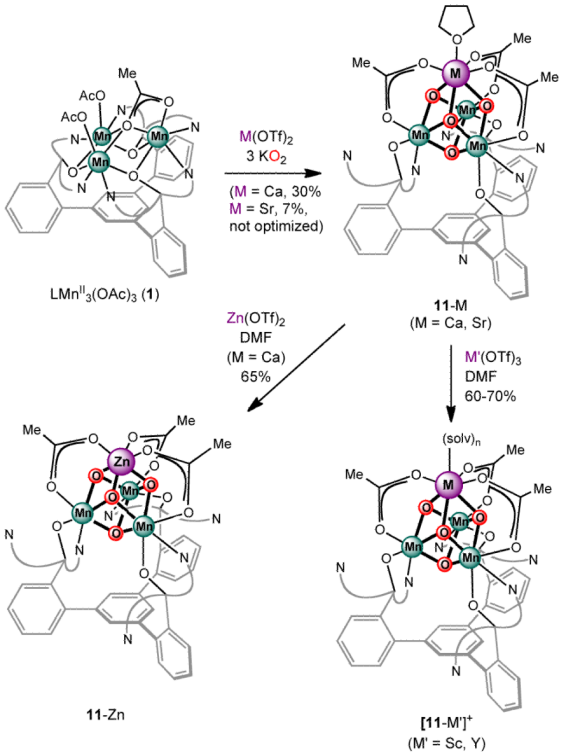

Scheme 7.
Synthesis of heterometallic tetraoxido cubane complexes.

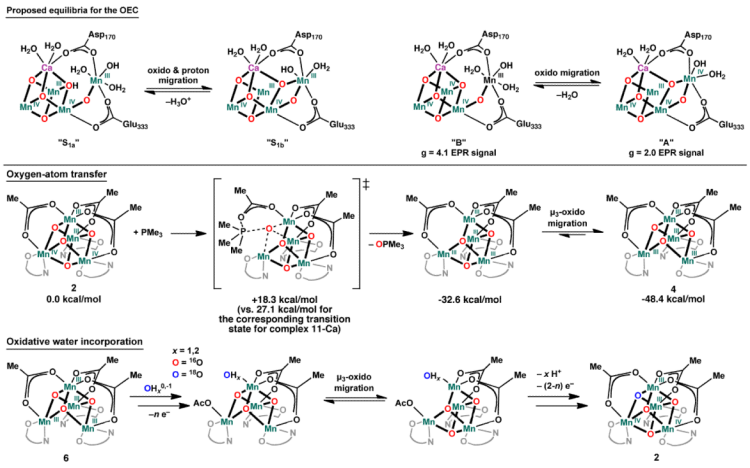

Scheme 8.

Proposed μ-oxido migration equilibria between OEC substates of S_1 and S_2 (top),[40-41] and proposed mechanisms for oxygen-atom transfer and oxidative water incorporation that depend on μ-oxido migration in model clusters (bottom).[135]